

# Enhanced electrochemical performance of xanthine biosensor by core - shell magnetic nanoparticles and carbon nanotube interface

Utkarsh Jain, Jagriti Narang and Nidhi Chauhan\*

Amity Institute of Nanotechnology (AINT), Amity University, Noida 201303, Uttar Pradesh, India

\*Corresponding author. Tel: (+91) 8130615833; E-mail: nidhichauhan2007@rediffmail.com

Received: 08 May 2015, Revised: 09 November 2015 and Accepted: 20 April 2016

## ABSTRACT

Xanthine oxidase (XOD) was extracted from bovine milk. Immobilization of extracted XOD was performed by covalently N-ethyl-N'-(3-dimethylaminopropyl) carbodiimide (EDC) and N-hydroxy succinimide (NHS) chemistry on core-shell magnetic nanoparticles (MNPs)/carboxylated multiwalled carbon nanotube (c-MWCNT) composite film. The film was electrodeposited on glass plate electrode (usually the surface of fluorine doped tin oxide (FTO)). In order to characterize nanocomposite modified FTO electrode, various methods including scanning electron microscopy (SEM), cyclic voltammetry (CV), Fourier transform infrared (FTIR), and electrochemical impedance spectroscopy (EIS) were performed. These methods were evaluated prior and following XOD immobilization. The working optimal conditions for instance 30 °C, +0.2 V vs. Ag/AgCl, sodium phosphate buffer at pH 7.0 were attributed for developing this biosensor. The linearity of the response upto 150 µM xanthine concentration, 0.05 µM (S/N = 3) detection limit and a response time within 3 s were obtained. The biosensor was stored at 4 °C and used above 100 times for a long period of 120 days. The loss of 50 % of activity was noticed. This fabricated biosensor was then employed determining xanthine in fish meat sample. Copyright © 2016 VBRI Press.

**Keywords:** Xanthine; xanthine oxidase; core-shell magnetic nanoparticles; multi-walled carbon nanotubes.

## Introduction

Xanthine (3, 7-dihydro-purine-2, 6-dione), a derivative obtained from hypoxanthine (a purine based compound) and guanine, is functionally catalyzed by guanine deaminase and xanthine oxidase. The pathological conditions which determine the elevated levels of xanthine in urine and blood samples are usually indicated by hyperuricemia, xanthineuria, gout and renal failure [1, 2]. Besides clinical diagnostics, xanthine is of great significance in food industry. High quality fish meat products in food industries require ATP of dead fish which consequently degrades into xanthine and increases during storage. Thus xanthine as an indicator for fish freshness is a compelling derivative product [3]. Presently, Xanthine is empirically analyzed by various methods including enzymatic colorimetric [4]; enzymatic fluorometric, fluorometric mass spectrometry fragmentography [5], HPLC [6] and hair like segment gas chromatography [7]. Although many pitfalls of these methods are widely noticed involving laborious procedure for sample preparation, need special reagents and requirement of costly equipments [8]. Considering sensitivity, rapid analysis and low cost delivery are advantageous parameters while using biosensing methods. Furthermore using biosensing technology, a simple method with electrochemical signals, provides a good alternative over various traditional analytical techniques [9, 10].

Integration of nanomaterials in biosensors can further enhance the properties of these biosensors. The

nanomaterials including nanoparticles, nanowires, nanotubes and nanochannels are previously incorporated in biosensing systems [11, 12]. Nanomaterials may generate novel interfaces which act as effective labels and amplify analysis. Furthermore, nanomaterials offer various advantages including stability, durability, better sensitivity, accuracy, detection range and faster response time. In few years, nanomaterials are of considerable interests manifesting unique properties in specific fields i.e., catalytic, electronic, and magnetic properties differ and usually applicable as compared to their larger counterparts. Oxide nanoparticles are immensely biocompatible and mainly applied to immobilize various biomolecules, whereas semiconductor nanoparticles are utilized to trace or label electrochemical analysis [13]. Although some nanoparticles are dismally and non-uniformly crystallized e.g. Iron oxide nanoparticles ( $\text{Fe}_3\text{O}_4$ ) and some nanocomposites [14], however several core-shell nanomaterials and nanocomposites are interestingly beneficial which are widely developed for various biosensor applications for instance the silica coating of nanoparticles. This is an effective tool as both core & shell structure can be utilized considering their valuable properties [15, 16]. Nano- $\text{Fe}_3\text{O}_4$  has hydrophilic surface and additionally act as a nanoscale electrode to enhance the transfer of electrons between the electrode surface and electro active Ferri/Ferro species. Since this combination form a permeable nano structure, the nano sized silica

seems a good biocompatible material for construction of various biosensors [17].

In the field of biosensing, the multiwalled carbon nanotubes (MWCNTs) are compelling component having their unique mechanical, electronic and structural and functional characteristics. Since MWCNTs possess plentiful surface area, splendid electrical conductance and superior chemical stability which make them a favorable constituent for protein immobilization [18, 19]. Together with metal nanoparticles, CNTs may serve as promising catalyst support forming a composite with a superb activity for some small molecules.

We hereby propose a precise construction of an amperometric xanthine biosensor thoroughly based upon electrochemical deposition of core-shell magnetic nanoparticles (MNPs) and MWCNT onto FTO electrode to form a composite layer of working electrode. After construction certain tools e.g., cyclic voltammetry and impedance spectroscopy were used to determine the electrochemical response of MNPs/MWCNT film. The analytical performance of the MNPs/MWCNT modified electrode was then evaluated with respect to detection limit, linearity, stability and reproducibility. To our knowledge, this is a first demonstration with the combination of MNPs and MWCNTs to achieve high selectivity with pure sensitivity for xanthine detection in fish.

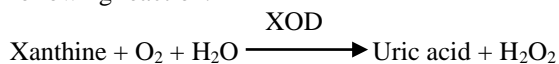
## Experimental

### Chemicals and reagents

Xanthine oxidase (XOD) (E.C.1.1.3.2) obtained from buttermilk (0.15 U/mg), xanthine extrapure, N-ethyl-N'-(3-dimethylaminopropyl) carbodiimide (EDC) and N-hydroxysuccinimide (NHS) from SRL, Mumbai, India were used. Carboxylated multi-walled carbon nanotubes (Functionalized MWCNT or c-MWCNT) (12 walls, length 15–30  $\mu\text{m}$ , Purity 90 %, Metal content: nil) from Intelligent Materials Pvt. Ltd., Panchkula (Haryana) India were used. Tetraethylorthosilicate (TEOS) and fluorine-tin-oxide (FTO) coated glass plate (100 mm  $\times$  100 mm  $\times$  2.3 mm) with a typical resistance of approximately  $\sim 7 \Omega/\text{Sq}$ . from Sigma-Aldrich, St. Louis, USA were purchased. Deionized water (DW) was used throughout the experiments. All chemicals and materials used were of only analytical reagent grade.

### XOD assay

XOD has previously been reported to catalyze the following reaction.



The rate of formation of urate from xanthine is determined by measuring increased absorbance at 290 nm due to uric acid. Bergmeyer *et al.* reported the assay for determining xanthine which is conducted in a test tube with certain modification based on xanthine oxidation to uric acid through XOD [20]. 1.8 mL of 50 mM sodium phosphate buffer (pH 7.0), 0.1 mL xanthine (0.15 mM) and 0.1 mL XOD (0.15 U/mg) were prepared. At 290 nm, an increase of absorbance was noticed compare to blank using

Spectrophotometry. The following formula is used to calculated activity:

$$\text{Units/mL} = \frac{\Delta A/\text{min} \times 1000 \times 3 \text{ mL} \times \text{df}}{1.22 \times 10^4 \times 0.1 \text{ mL}}$$

(where, total vol. of the reaction mixture (mL) = 3 mL, Extinction Coeff. of uric acid =  $1.22 \times 10^4 \text{ cm}^{-1}$ , volume of enzyme used (mL) = 0.1 mL, df = Dilution factor)

\*One unit will convert 1.0 n mole of xanthine to uric acid per min. per mL at pH 7.5 at 25  $^\circ\text{C}$ .

### Preparation of MNPs

A typical procedure is followed for synthesis of MNPs. In this process, 0.4 M hydrochloric acid and 0.7 M ammonia solution were given  $\text{N}_2$  for 10 min. Then 8.5 g  $\text{FeCl}_3 \cdot 6\text{H}_2\text{O}$  and 3 g  $\text{FeCl}_2 \cdot 4\text{H}_2\text{O}$  were mixed in 38 ml of 0.4 M hydrochloric acid. Following mixing, 375 ml  $\text{NH}_3$  solution was added under vigorous stirring at room temperature. The solution was stirred for half an-hour and the precipitates were extracted via magnetic force. After washing 3 times with water, the precipitates were then diluted with 150 ml DW. Following, magnetic MNPs core was coated by silica. The prepared 20 ml of MNPs was added to 200 ml of Isopropyl alcohol and further sonicated for 20-25 min. After sonication, 10 ml ammonia solution (28 wt.%), PEG (5.36 g) with 20 ml water and 1.2 ml TEOS were merged and the solution was kept for another 24 h with continuous stirring at room temperature. Once the reaction was completed, the solution was centrifuged at 4000 rpm for 5 min and then further sonicated twice with ethanol and distilled water. The lyophilization was applied to collect the core-shell MNPs.

### Deposition of MNPs onto c-MWCNTs

The deposition of MNPs onto c-MWCNTs was prepared by Jain *et al.*, 2015 with small modifications [21]. First, 0.265 g MNPs was dispersed into 200 mL of DW by stirring. After adding 1.0 mg of c-MWCNTs to the solution, ultrasonic treatment was given for 10 min. Finally, 0.4 mol  $\text{L}^{-1}$  sodium hydroxide was given drop-by-drop into the solution to make pH of 7.0. MNPs/c-MWCNTs solution was stirred for about 30 min and then desiccated for 2 h at 50-55  $^\circ\text{C}$ . The solution was centrifuged at 5000 x g for 10-15 min for separating the product in the mixture [22]. A black colored precipitate was obtained which was washed with the DW maintaining pH 7.0. Pure methanol treatment was given to MNPs/c-MWCNTs composites the product was then desiccated for 6 h at 50  $^\circ\text{C}$ .

### Construction of MNPs/c-MWCNT modified FTO electrode

An electrochemical cleaning of FTO electrode was done by setting the electrode having potential range of +1.6 and  $-0.4 \text{ V}$  in 0.5 mol  $\text{L}^{-1}$   $\text{H}_2\text{SO}_4$ . The process is stopped once a stable voltammogram was acquired. The electrodeposition of MNPs/c-MWCNTs nanocomposite onto FTO electrode was formulated in an electrochemical cell connected to potentiostat/galvanostat. FTO electrode in a 25 mL solution containing 22 mL electrolyte (2.5 mmol  $\text{L}^{-1}$   $\text{K}_3\text{Fe}(\text{CN})_6/\text{K}_4\text{Fe}(\text{CN})_6$  [1:1]) and 3 mL nanomaterial was

immersed and 20–30 cycles of  $-0.2$  to  $+0.6$  V were applied at a fast scan rate of  $50 \text{ mV s}^{-1}$ . The unbound nanomaterial was removed from prepared MNPs/c-MWCNTs/FTO electrode by wiping completely with DW and then stored it in petri plate at  $4^\circ\text{C}$ .

#### *XOD enzyme immobilization on FTO electrode coated with MNPs/c-MWCNT composite film*

A covalent immobilization of enzyme XOD was performed on FTO electrode coated with MNPs/c-MWCNT composite film by EDC and NHS coupling explained by Rahman *et al.* with some modifications [23]. Firstly,  $0.1 \text{ M}$  sodium phosphate buffer were used to activate a free and unbound  $-\text{COOH}$  groups of MNPs/c-MWCNT composite film by dipping in it with the pH of 7.5 having EDC and NHS of  $10 \text{ mM}$  concentration for the period of approximately 6 h. Excess of EDC and NHS was thoroughly washed away by  $0.05 \text{ M}$  sodium phosphate buffer (pH 7.4). In last, electrode was treated with EDC–NHS and further incubated in  $5 \text{ mL}$   $0.05 \text{ M}$  sodium phosphate buffer of pH 7.4 having XOD ( $24 \text{ U}$ ) for 3 h at  $4^\circ\text{C}$ . The electrode was then washed with same concentration of sodium phosphate buffer (pH 7.4). The immobilized enzyme electrode was then dried and kept in refrigerator at  $4^\circ\text{C}$ .

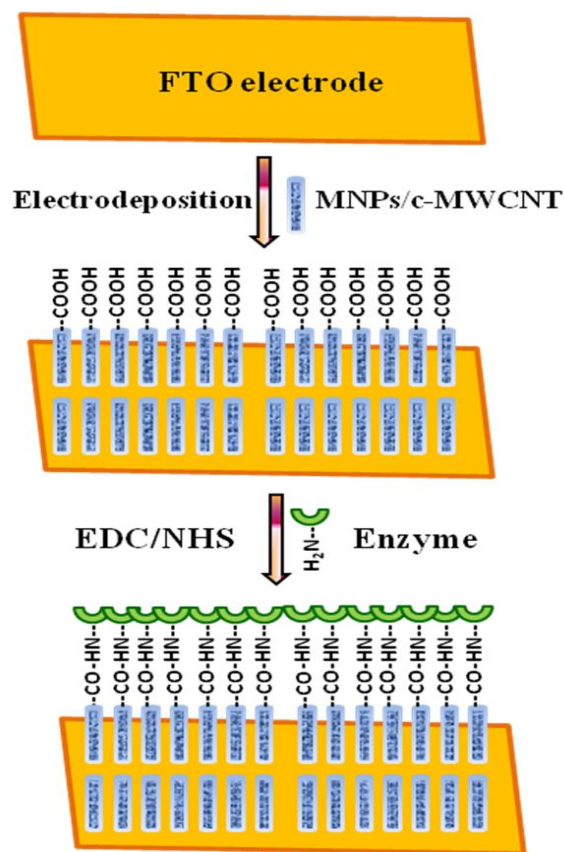
#### *Measurement by cyclic voltammetric for testing xanthine biosensor*

XOD/MNPs/c-MWCNT/FTO electrode (working electrode) was evaluated in the form of cyclic voltammogram (CV). Potentiostat–galvanostat ranging  $-0.4$  to  $+0.4 \text{ V}$  working electrode vs Ag/AgCl as reference and Pt wire as counter electrode were submerged in  $15 \text{ mL}$  ( $0.05 \text{ M}$ ) of sodium phosphate buffer having pH 7.5 which contain  $0.15 \text{ mM}$  xanthine ( $0.5 \text{ mL}$ ). The highest response was observed at  $+0.2 \text{ V}$  considering this voltage as a standard for subsequent amperometric studies. In next studies, the modified electrode (XOD/MNPs/c-MWCNT/FTO electrode), the reference electrode and the counter electrode were all together submerged in  $25 \text{ mL}$   $0.05 \text{ M}$  sodium phosphate buffer having pH 7.4. The xanthine solution at various concentrations was added to start reaction in the mixture and the generated current (mA) was measured at  $+0.2 \text{ V}$ .

#### *Optimization and evaluation of xanthine biosensor*

The conditions which experimentally affect biosensor response were thoroughly studied. These conditions are incubation temperature, influence of pH, time of response and xanthine concentration as a substrate. Taking into account of optimum pH, the varied ranges from 3.0 to 8.0 at an interval of 0.5 were considered. Likewise, an optimum temperature was decided while the reaction mixture was incubated at various temperatures ranging from  $20$ – $50^\circ\text{C}$  having difference of  $5^\circ\text{C}$ . The incubation time between 1–10 s with 1 s intervals were evaluated. At various xanthine concentrations for biosensor response measurements were estimated ranging from  $0.05 \mu\text{M}$  to  $120 \mu\text{M}$  with the difference in concentration of  $20 \mu\text{M}$ .

Finally, the biosensor performance was recorded based on their limit of detection, linear range, recovery, repeatability (precision), reproducibility and stability during storage.



**Scheme 1.** Schematic representation of stepwise amperometric xanthine biosensor fabrication process.

#### *Amperometric determination of xanthine in fish meat*

Firstly, Labeo fish was minced and then homogenized in  $10 \text{ mL}$   $0.5 \text{ M}$   $\text{HClO}_4$  making a fine paste for attaining proteins present in the sample. Centrifugation at  $4000 \text{ rpm}$  for 5–10 min was performed for the denatured sample proteins after stirred for about 10 min. The supernatant was separated and adjusted for pH of 7.0 with NaOH. After 10 times dilution, the supernatant (fish meat extract) of denatured solutions were divided into two segments. One segment was kept at room temperature and another one was used immediately. In order to determine xanthine content/concentration in fish meat extract, the procedure followed was same as described previously in sensor's response measurement. This measurement was taken for xanthine sample under optimal working conditions. The calculation of xanthine content in the sample was done by interpolating a calibration curve between xanthine concentrations vs current (mA).

## Results and discussion

The preparation of MNPs/c-MWCNT nanocomposite on FTO electrode was performed by a chemically simple method. **Scheme 1** illustrates MNPs coated on outer walls of c-MWCNTs with other nanoparticles [21, 22]. The

surfaces of MWCNTs contain carboxyl groups bind with  $-NH_2$  groups present on the surface of XOD. Once decorated, XOD was covalently immobilized on MNPs/c-MWCNT composite film by applying EDC-NHS chemistry. This EDC-NHS is mainly used for activating the free  $-COOH$  groups available on MNPs/c-MWCNT composite film.

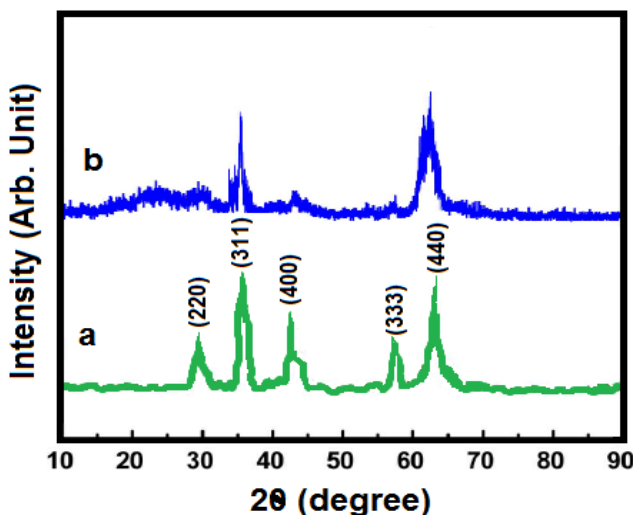


Fig. 1. XRD pattern for (a) MNPs and (b) core-shell MNPs.

#### Characterization of MNPs

The XRD patterns obtained for the samples exhibit high crystalline peaks indicating an enormous similarity with the standard crystal phase of magnetite (JCPDS No. 894319, 19-0629). The peaks indicating 15u to 35u represents the presence of amorphous-SiO<sub>2</sub> [24].

Furthermore, the same samples of MNPs used for getting XRD patterns were taken for TEM. Fig. 1 shows high resolution electron microscope image acquired by TEM which confirms that particles are appeared in a single crystalline form (Fig. 2). These particles are mainly spherical or compact in shape. After detailed analysis of TEM image, 10 to 40 nm of particle size was observed which possess an average size of  $25 \pm 1.5$  nm.

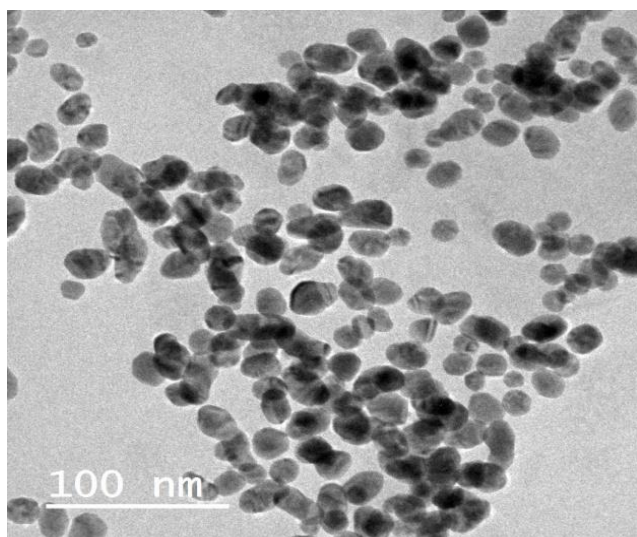


Fig. 2. TEM image of core-shell MNPs of an average diameter of 25 nm.

#### Surface characterization by SEM

The SEM of FTO electrode, MNPs/c-MWCNT/FTO electrode and XOD/MNPs/c-MWCNT/FTO electrode were used to study the shapes and structures present on the surface (Fig. 3). A uniform surface was observed for bare FTO electrode (Fig. 3a), a uniform but granular morphology was noticed for the MNPs/c-MWCNT/FTO electrode revealing a uniform distribution of MNPs in MWCNT network (Fig. 3b). Once immobilization of XOD was completed, a covalent linking between MNPs/c-MWCNT with XOD was occurred indicating an alteration of structural morphology of MNPs/c-MWCNT/FTO into the regular form (Fig. 3c).

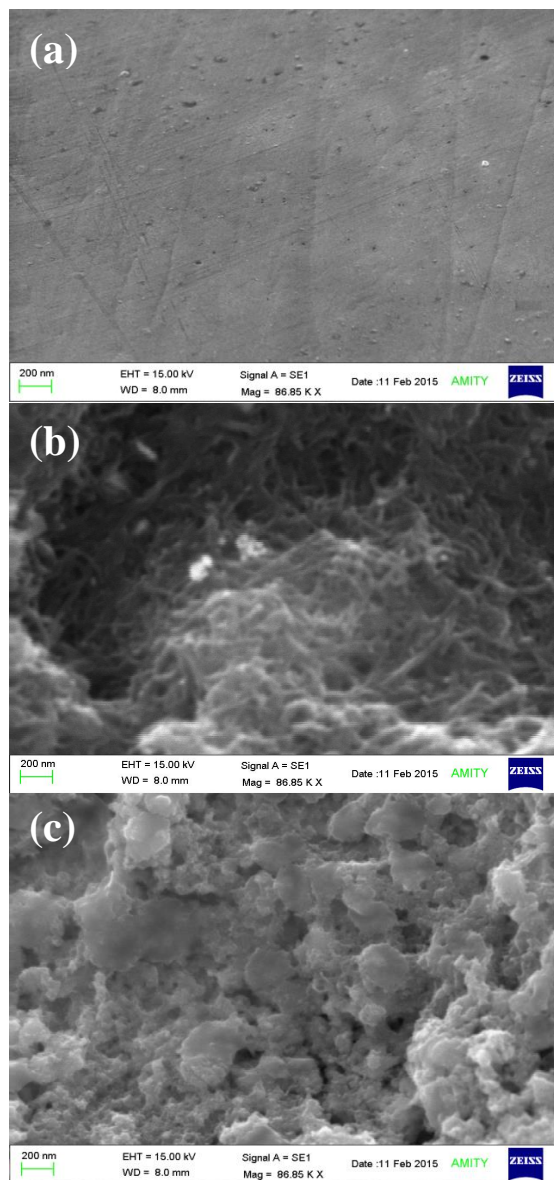
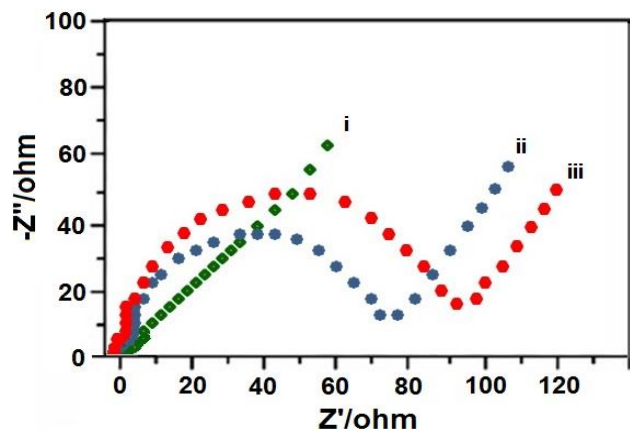


Fig. 3. Scanning electron micrographs of (a) bare FTO electrode, (b) MNPs/c-MWCNT/FTO electrode and (c) XOD/MNPs/c-MWCNT/FTO electrode.

#### Electrochemical impedance spectroscopic (EIS) studies

Electrochemical impedance spectroscopic (EIS) studies contribute significantly to determine changes occurred during the process of fabrication of the electrode surface

and were utilized to analyze the immobilization of enzyme on MNPs/c-MWCNT/FTO electrode. The charge transfer resistance (RCT) was equivalent to the diameter of the semicircle section of frequencies of the Nyquist plot determining the transfer of electron and redox probe kinetics during interface of electrodes. The Warburg diffusion process is shown as linear part at lower frequencies [25]. The Nyquist plot (Fig. 4) is presented for EIS studies showing a plain/bare FTO electrode (curve a), MNPs/c-MWCNT/FTO electrode (curve b) and enzyme/MNPs/c-MWCNT/FTO electrode (curve c). The buffer and probe used in this studies were 0.05 M sodium phosphate buffer (pH 7.4) and 5 mM  $K_3Fe(CN)_6/K_4Fe(CN)_6$  (1:1) as a redox probe. The RCT value for the bare FTO electrode was 108  $\Omega$  however MNPs/c-MWCNT and XOD/MNPs/c-MWCNT/FTO electrodes were 75  $\Omega$  and 95  $\Omega$ . Since RCT of MNPs/c-MWCNT/FTO electrode (curve b) was lesser as compared to FTO electrode (curve a), this imparts that FTO electrode has a high electron transfer rate with reduced resistance. The MNPs immobilized onto the c-MWCNTs was layered as a thin MNPs film. The fact suggests that an improvement of c-MWCNT was occurred which makes the composite showing more active sites for electrochemical reactions with a high capacitance by FTO electrode. The charge-transfer of the composite enhances conductivity and reduces resistance. The RCT of XOD/MNPs/c-MWCNT/FTO electrode (curve c) was increased whereas the RCT of MNPs/c-MWCNT/FTO electrode was decreased. Since the biological samples for instance enzymes used in this study have poor electron transfer rate at low frequencies, therefore RCT is increased because of obstacle in electron transfer confirming the binding of XOD onto MNPs/c-MWCNT composite.



**Fig. 4.** Nyquist plot of electrochemical impedance spectra for FTO electrode (curve i), MNPs/c-MWCNT/FTO electrode (curve ii) and XOD/MNPs/c-MWCNT/FTO electrode (curve iii) in 0.05 M sodium phosphate buffer (pH 7.5) containing 5 mM  $K_3Fe(CN)_6/K_4Fe(CN)_6$  (1:1) as a redox probe.

#### Construction of XOD/MNPs/c-MWCNT modified FTO electrode

The construction of an electrochemical xanthine biosensor was performed by immobilizing XOD on MNPs/c-MWCNT which is then electrodeposited on the surface of

FTO. The prepared construct serves as a working electrode with Ag/AgCl as reference and Pt wire used as an auxiliary electrode. The potential peaks of MNPs/c-MWCNT/FTO electrode were not changed for cycling between  $-0.4$  and  $+0.4$  V. The morphological properties of film deposited on FTO were stable. The same electrochemical behavior of composite material was observed for MNPs and c-MWCNT.

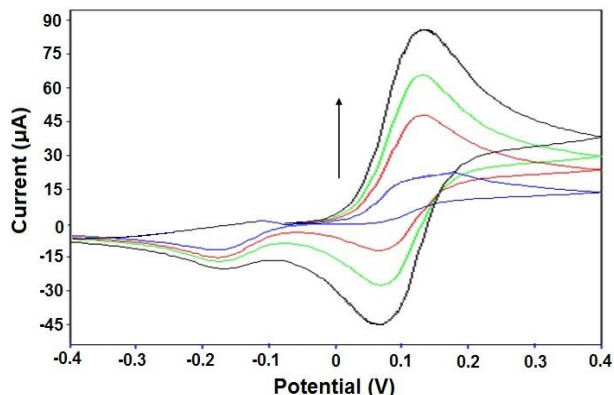


**Fig. 5.** Cyclic voltammograms, (a) bare FTO electrode, (b) c-MWCNT/FTO electrode, (c) MNPs/c-MWCNT/FTO electrode and (d) XOD/MNPs/c-MWCNT/FTO electrode in pH 7.5 sodium phosphate containing 0.1 mM xanthine. Scan rate: 50  $mV s^{-1}$ .

Since in this improved amperometric biosensor the covalent immobilization of XOD was achieved on MNPs/c-MWCNT/FTO electrode, the performance of the biosensor was evaluated. During stepwise modification, the performance was evaluated for the working FTO electrode in 0.05 M phosphate buffer (pH 7.5). The CV of FTO electrode, c-MWCNT/FTO electrode, MNPs/c-MWCNT/FTO electrode and XOD/MNPs/c-MWCNT/FTO electrode in presence of 100  $\mu L$  of xanthine (0.1 mM) in sodium phosphate buffer (pH 7.5) at a scan rate of 50  $mV s^{-1}$  was shown in Fig. 5. There was no peak observed for FTO electrode (curve a) in phosphate buffer while injecting 100  $\mu L$  of xanthine into reaction cell. The cyclic voltammogram of c-MWCNT/FTO electrode and MNPs immobilized onto the c-MWCNTs identified an oxidation peak at 42 and 57  $\mu A$  (curve b and c), respectively. c-MWCNT is used as a useful adsorbent for heavy metal ions and its solutions [26]. In addition, the voltammogram represents a major reduction peak where there is a process for titanium reduction and the current decreases by diffusion. An oxidation peak at 87  $\mu A$  (vs Ag/AgCl) (curve d) was recorded by CV of XOD/MNPs/c-MWCNT/FTO electrode.

The modification of the bare FTO electrode with conductive MNPs/MWCNTs resulted in a higher  $I_p$  and smaller  $\Delta E_p$  owing to an increase of potent surface. The  $I_p$  of the XOD/MNPs/MWCNT modified FTO electrode was even higher illustrating oxidation of xanthine which is catalyzed by the immobilized XOD on the MNPs/MWCNT/FTO surface.

#### Optimization of experimental conditions

Optimization studies were conducted using linear sweep voltammetry (LSV) on various factors which effects

incubation, pH, response time and temperature. Whether the response current of the XOD/MNPs/c-MWCNT/FTO electrode is affected by the pH was studied between 3.0 and 8.0 at an interval of 0.5. The response current was elevated from 3.0 to 7.5 and then decreased. The recorded maximum current was at pH 7.0. Therefore, the pH 7.0 was considered favorable for optimal activity of immobilized XOD to soluble XOD [20]. To ensure the optimization, the effect of temperature on biosensor was thoroughly studied. The response current was reached at maximum on approximately 30 °C and then reduced with increased temperature. The present biosensor showed a maximum response (comparatively faster) within 3 s.

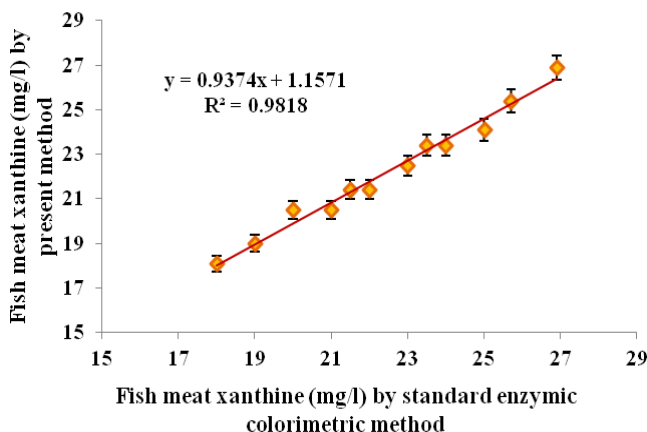


**Fig. 6.** Correlation between fish meat extract (mg/L) determinations by standard enzymic colorimetric method (x) and present biosensor method (y).

A linear correlation between biosensor response and xanthine concentration was obtained which was in the range of concentration between 0.05  $\mu\text{M}$  to 150  $\mu\text{M}$ . Although it was reported constant after 150  $\mu\text{M}$ . There are many anodic and cathodic peaks associated with the figure due to presence of electrolyte i.e.  $\text{K}_3\text{Fe}(\text{CN})_6/\text{K}_4\text{Fe}(\text{CN})_6$  (1:1), which acts as a redox probe. The current peaks are associated with desorption of ferri/ferro from the modified FTO electrode surface. Some peaks are related with the reduction of oxygen and/or species.

#### Evaluation of prepared xanthine biosensor

A linear correlation between xanthine concentration ranging from 0.05 to 150  $\mu\text{M}$  and current (A) was acquired stipulating construction of a better biosensor as compared to zinc oxide nanoparticle (ZnO-NPs)-polypyrrole (PPy) composite film modified Pt electrode (0.8 to 40  $\mu\text{M}$ ) [2], ZnO-NPs/chitosan/c-MWCNT/polyaniline modified Pt electrode (0.1 to 100  $\mu\text{M}$ ) [27], Au/polypyrrole (AuPPy) nanocomposites modified Pt electrode (0.4 to 100  $\mu\text{M}$ ) [28], double walled carbon nanotube (DWCNT) modified carbon paste electrode (2 to 50  $\mu\text{M}$ ) [29], CNT modified carbon paste electrode (1–100  $\mu\text{M}$ ) [30], chitosan bound Au coated iron nanoparticles (CHIT/Fe-NPs@Au)/PGE (0.1–300  $\mu\text{M}$ ) [31] and Self-assembled biotinylated phospholipid membrane (20 to 100  $\mu\text{M}$ ) [32]. The range of 0.05  $\mu\text{M}$  (S/N = 3) was the detection limit obtained for this biosensor which is reportedly lower compared to detection limit of ZnO-NPs-polypyrrole (PPy) composite film

modified Pt electrode (0.8  $\mu\text{M}$ ) [2], ZnO-NPs/ chitosan/c-MWCNT/polyaniline modified Pt electrode (0.1  $\mu\text{M}$ ) [27], Au/polypyrrole (AuPPy) nanocomposites modified Pt electrode (0.4  $\mu\text{M}$ ) [28], iron (III) mesotetraphenylporphyrin nanoparticles modified glassy carbon (1  $\mu\text{M}$ ) [33], DWCNT modified carbon paste electrode (2  $\mu\text{M}$ ) [29] & CNT modified carbon paste electrode (0.75  $\mu\text{M}$ ) [30]. Xanthine was added separately to study analytical recovery. Thus 0.1 mL of xanthine solution (10 mg L<sup>-1</sup>, 20 mg L<sup>-1</sup>) in fish meat extract was added exogenously. Once the xanthine was added in the fish meat extract, the concentration was calculated by measuring through our method before and after addition. The measurement was carried out immediately. The % recoveries of added xanthine were 96.5 $\pm$ 1.2 % and 98.4 $\pm$ 1.5 %. The more recovery reveals a high analytical reliability of our method. In order to examine the accuracy of our method, the values of xanthine in fish samples (n=12) were compared with enzymatic colorimetric method (x) to our method (y). The comparison of xanthine concentrations of these two methods showed a high correlation ( $R^2 = 0.9818$ , significant at 1 % level) (Fig. 6) indicating a good accuracy.

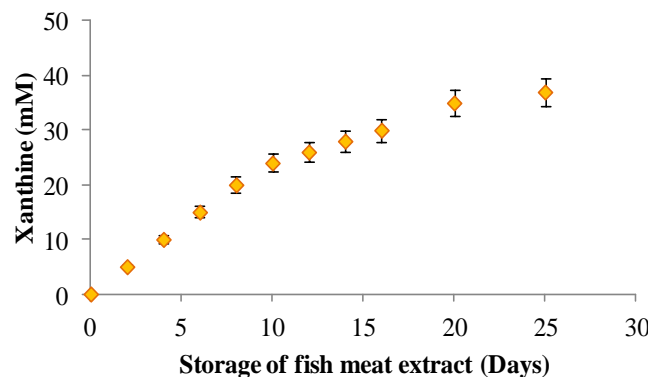


**Fig. 7.** Determination of xanthine in fish meat by xanthine biosensor based on XOD/MNPs/c-MWCNT/FTO electrode during storage at room temperature (25 $\pm$ 5°C).

Comparatively, a higher detection limit was obtained by the present method than colorimetric method. The other important characteristics including reproducibility and repeatability of our method were evaluated. The significant result was obtained for same fish sample when the xanthine concentration was checked in a day for five times (within batch). Thereafter the sample was stored at 4 °C for one week (between batches). The results showed the consistency over a long period of time. The coefficients of variation (CV) within and between the batch for fish sample determination were reported by <4.7 % and <5.6 % showing a high reproducibility with true reliability of our method.

#### Xanthine concentration in fish meat

The xanthine concentration in fish meat was calculated using prepared biosensor at different storage times up to 25 days always at room temperature. The xanthine concentration was increased from 0.9 to 37.6 mM/g during storage. The concentration was doubled after 4 days (Fig. 7).

### Examine stability of electrode in long-term

To evaluate the storage stabilities in long-term, the activity of XOD/MNPs/c-MWCNT/FTO electrode was measured in terms of the storage time. Reaction buffer was prepared to wash enzyme electrode for 2 – 3 times so as to reuse and avoiding a possibility of blocking of the electrode by various soluble proteins present in fish meat extract. The initial activity of electrode was measured and the loss of initial activity for 100 regular uses during experimental 120 days was determined giving only 50 % of initial activity (Fig. 8), resulting a higher than previously reported XOD biosensors ZnO-NPs–polypyrrole (PPy) composite film modified Pt electrode (100 days) [2], ZnO-NPs/ chitosan/c-MWCNT/polyaniline modified Pt electrode (30 days) [27] and Au/polypyrrole (AuPPy) nanocomposites modified Pt electrode (100 days) [29]. Thus an efficient coupling between enzyme and nanocomposite material was noticed and resulting in retaining the activity of immobilized XOD. In addition, because of covalent coupling, the leaking out of the FTO electrode is prevented.

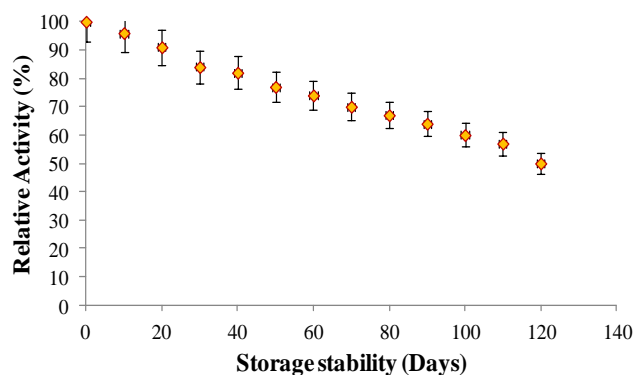


Fig. 8. XOD/MNPs/c-MWCNT/FTO electrode: Response for the effect of storage stability.

### Conclusion

In summary, we have successfully designed a signal amplified electrochemical enzyme sensor for xanthine based on the synergistic catalysis of XOD and MNPs/c-MWCNT nanostructures. The fabricated XOD/MNPs/c-MWCNT/FTO electrode exhibited low detection limit (0.05  $\mu\text{M}$ ), wide linear range (0.05 to 150  $\mu\text{M}$ ), high stability (120 days) and a faster response time which is within 3s at +0.2 V vs Ag/AgCl potential. We establish an efficient electrocatalytic activity and stability with biological compatibility of MNPs/c-MWCNT which would enhance our understanding to far going applications of biosensors.

### Acknowledgements

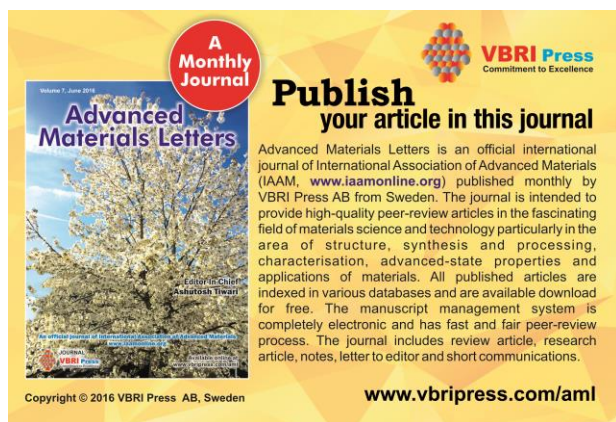
The research grant was provided by Science and Engineering Research Board (SERB), New Delhi. A Young Scientist Scheme (Fast Track) was awarded to Dr. Nidhi Chauhan heartily acknowledging Department of Science & Technology (DST).

### Reference

1. Edwards, N. L.; *Rheumatol.* **2009**, *48*, 15.  
DOI: [10.1093/rheumatology/kep088](https://doi.org/10.1093/rheumatology/kep088)
2. Devi, R.R.; Thakur, M.; Pundir, C.S.; *Biosens. Bioelectron.* **2011**, *26*, 3420.

3. Shan, D.; Wang, Y.; Xue, H.; Cosnier, S.; *Sens. Actuators*, **2009**, *136*, 510.  
DOI: [10.1016/j.snb.2008.10.012](https://doi.org/10.1016/j.snb.2008.10.012)
4. Pu, W.; Zhao, H.; Wu, L.; Zhao, X.; *Microchim. Acta*, **2015**, *182*, 395.  
DOI: [10.1007/s00604-014-1342-2](https://doi.org/10.1007/s00604-014-1342-2)
5. Olojoa, R.O.; Xiab R.H.; Abramsona, J. J.; *Anal. Biochem.* **2005**, *339*, 338.  
DOI: [10.1016/j.ab.2005.01.032](https://doi.org/10.1016/j.ab.2005.01.032)
6. Papadoyannis, I.N.; Samanidou, V. F.; Geoga, K.A.; *J. Liq. Chromatogra. Relat. Technol.* **1996**, *19*, 2559.  
DOI: [10.1080/10826079608014038](https://doi.org/10.1080/10826079608014038)
7. Renata, S.; Pagliarussi, L.; Luis, A. P.; Freitas, L.; Bastos, J. K.; *J. Sep. Sci.* **2002**, *25*, 371.  
DOI: [10.1002/1615-9314\(20020401\)25:5/6<371](https://doi.org/10.1002/1615-9314(20020401)25:5/6<371)
8. Dodevska1, T.; Horozova, E.; Dimcheva, N.; *Cent. Eur. J. Chem.* **2010**, *8*, 19.  
DOI: [10.2478/s11532-009-0102-3](https://doi.org/10.2478/s11532-009-0102-3)
9. Mu, S.; Shi, Q.; *Biosens. Bioelectron.* **2013**, *47*, 429.  
DOI: [10.1016/j.bios.2013.03.036](https://doi.org/10.1016/j.bios.2013.03.036)
10. Kalimuthu, P.; Leimkühler, S.; Bernhardt, P. V.; *Anal. Chem.* **2012**, *84*, 10359.  
DOI: [10.1021/ac3025027](https://doi.org/10.1021/ac3025027)
11. Chauhan, N.; Pundir, C.S.; *Biosens. Bioelectron.* **2014**, *61*, 1.  
DOI: [10.1016/j.bios.2014.04.048](https://doi.org/10.1016/j.bios.2014.04.048)
12. Chauhan, N.; Narang, J.; Sunny, Pundir, C. S.; *Enz. Microb. Technol.*, **2013**, *52*, 265.  
DOI: [10.1016/j.enzmictec.2013.01.006](https://doi.org/10.1016/j.enzmictec.2013.01.006)
13. Luo, X.; Morrin, A.; Killard, A.J.; Smyth, M.R.; *Electroanal.* **2006**, *18*, 319.  
DOI: [10.1002/elan.200503415](https://doi.org/10.1002/elan.200503415)
14. Moser, A.; Takano, K.; Margulies, D.T.; Albrecht, M.; Sonobe, Y.; Ikeda, Y.; Sun, S.; Fullerton, E.E.; *J. Phys. D: Appl. Phys.* **2002**, *35*, R157.  
DOI: [10.1088/0022-3727/35/19/201](https://doi.org/10.1088/0022-3727/35/19/201)
15. Md. N.; Islam, M.; Abbas, B.; Sinha, J.-R.; Joeng, C.G.; Kim, *Electron. Mater. Lett.* **2013**, *9*, 817.  
DOI: [10.1007/s13391-013-6019-1](https://doi.org/10.1007/s13391-013-6019-1)
16. Wu, W.; He, Q.; Jiang, C.; *Nanoscale. Res. Lett.* **2008**, *3*, 397.  
DOI: [10.1007/s11671-008-9174-9](https://doi.org/10.1007/s11671-008-9174-9)
17. Qhobosheane, M.; Santra, S.; Zhang, P.; Tan, W.; *Analyst* **2001**, *126*, 1274.  
DOI: [10.1039/B101489G](https://doi.org/10.1039/B101489G)
18. Chauhan, N.; Pundir, C.S.; *Anal. Biochem.* **2011**, *413*, 97.  
DOI: [10.1016/j.ab.2011.02.007](https://doi.org/10.1016/j.ab.2011.02.007)
19. Chauhan, N.; Pundir, C.S.; *Anal. Chim. Acta*, **2011**, *701*, 66.  
DOI: [10.1016/j.aca.2011.06.014](https://doi.org/10.1016/j.aca.2011.06.014)
20. Shintani, H.; *Pharm. Anal. Acta*, **2013**, *S7*, 2153.  
DOI: [10.4172/2153-2435.S7-004](https://doi.org/10.4172/2153-2435.S7-004)
21. Jain, U.; Narang, J.; Rani, K.; Burna, Sunny, Chauhan, N.; *RSC Adv.* **2015**, *5*, 29675.  
DOI: [10.1039/c5ra00050e](https://doi.org/10.1039/c5ra00050e)
22. Chauhan, N.; Pundir, C.S.; *Electrochim. Acta*, **2012**, *67*, 79.  
DOI: [10.1016/j.electacta.2012.02.012](https://doi.org/10.1016/j.electacta.2012.02.012)
23. Rahman, M.M.; Muhammad, J.A.; Shiddiky, Rahman, M.A.; Shim, Y.B.; *Anal. Biochem.* **2009**, *384*, 159.  
DOI: [10.1016/j.ab.2008.09.030](https://doi.org/10.1016/j.ab.2008.09.030)
24. Song, N.-N.; Yang, H.-T.; Liu, H.-L.; Ren, X.; Ding, H.-F.; Zhang, X.-Q.; Cheng, Z.-H.; *Sci. Rep.* **2013**, *3*, 3161.  
DOI: [10.1038/srep03161](https://doi.org/10.1038/srep03161)
25. Feng, J.J.; Zhao, G.; Xu, J.J.; Chen, H.Y.; *Anal. Biochem.* **2005**, *342*, 280.  
DOI: [10.1016/j.ab.2005.04](https://doi.org/10.1016/j.ab.2005.04)
26. Kuo, C.-Y.; Lin, H.-Y.; *Desalination*, **2009**, *249*, 792.  
DOI: [10.1016/j.desal.2008.11.023](https://doi.org/10.1016/j.desal.2008.11.023)
27. R.; Devi, S.; Yadav, C.S.; Pundir, *Analyst*, **2012**, *137*, 754.  
DOI: [10.1039/c1an15838d](https://doi.org/10.1039/c1an15838d)
28. Devi, R.; Yadav, S.; Pundir, C.S.; *Colloids Surf. A*, **2012**, *394*, 38.  
DOI: [10.1016/j.colsurfa.2011.11.021](https://doi.org/10.1016/j.colsurfa.2011.11.021)
29. Anik, U.; Çevik, S.; *Microchim. Acta*, **2009**, *166*, 209.  
DOI: [10.1007/s00604-009-0190-y](https://doi.org/10.1007/s00604-009-0190-y)
30. Torres, A.C.; Ghica, M.E.; Brett, C.M.; *Anal. Bioanal. Chem.* **2013**, *405*, 3813.  
DOI: [10.1007/s00216-012-6631-1](https://doi.org/10.1007/s00216-012-6631-1)

31. Devi, R.; Yadav, S.; Nehra, R.; Yadav, S.; Pundir, C. S.; *J. Food Eng.* **2013**, *115*, 207.  
DOI: [10.1016/j.jfoodeng.2012.10.014](https://doi.org/10.1016/j.jfoodeng.2012.10.014)
32. Rehak, M.; Snejdarkova, M.; Otto, M.; *Biosens. Bioelectron.* **1994**, *9*, 337.  
DOI: [10.1016/0956-56639480033-2](https://doi.org/10.1016/0956-56639480033-2)
33. Li, X.H.; Xie, Z.H.; Min, H.; Xian, Y.Z.; Tongjin, L.; *Anal. Lett.* **2008**, *41*, 456.  
DOI: [10.1080/00032710701567055](https://doi.org/10.1080/00032710701567055)



**A Monthly Journal**

**Publish your article in this journal**

Advanced Materials Letters is an official international journal of International Association of Advanced Materials (IAAM, [www.iaamonline.org](http://www.iaamonline.org)) published monthly by VBRI Press AB from Sweden. The journal is intended to provide high-quality peer-review articles in the fascinating field of materials science and technology particularly in the area of structure, synthesis and processing, characterisation, advanced-state properties and applications of materials. All published articles are indexed in various databases and are available download for free. The manuscript management system is completely electronic and has fast and fair peer-review process. The journal includes review article, research article, notes, letter to editor and short communications.

Copyright © 2016 VBRI Press AB, Sweden

[www.vbripress.com/aml](http://www.vbripress.com/aml)